CHINESE JOURNAL OF CATALYSIS
Volume 32, Issue 8, 2011
Online English edition of the Chinese language journal

Available online at www.sciencedirect.com
ScienceDirect

Cite this article as: Chin. J. Catal., 2011, 32: 1349–1356.

RESEARCH PAPER

Structural Characterization and Photocatalytic Activity of Hydrothermally Synthesized Mesoporous TiO_2 for 2,4,6-Tribromophenol Degradation in Water

LUO Haiying[1,2], NIE Xin[1,2], LI Guiying[1], LIU Jikai[1,2], AN Taicheng[1,*]

[1]State Key Laboratory of Organic Geochemistry, Guangdong Key Laboratory of Environmental Resources Utilization and Protection, Guangzhou Institute of Geochemistry, Chinese Academy of Sciences, Guangzhou 510640, Guangdong, China
[2]Graduate University of Chinese Academy of Sciences, Beijing 100049, China

Abstract: Well defined mesoporous TiO_2 (M-TiO_2) nanocrystallites were prepared by the hydrothermal method using polypropylene glycol (PPG) as template. The method differs from traditional methods in the use of an acetic acid aqueous solution instead of the conventional hydrolysis inhibitors and acid catalysts. The morphology and microstructures of M-TiO_2 were characterized by X-ray diffraction, thermogravimetric and differential thermogravimetric, scanning electron microscopy, and nitrogen adsorption-desorption. The effects of the synthesis process, template reagent content, and calcination temperature on the microstructure and photocatalytic activity were investigated. The relationship between the microstructure of M-TiO_2 and its photocatalytic activity was studied by the photocatalytic degradation of 2,4,6-tribromophenol in water under UV irradiation. M-TiO_2 with a regular channel structure, large pore size, and high specific surface area was successfully synthesized. The M-TiO_2 synthesized by the hydrothermal method and calcined at 400 °C that used a PPG content of 20% gave the highest photocatalytic activity, and completely degraded 100 μmol/L 2,4,6-tribromophenol within 1 h.

Key words: mesoporous titania; hydrothermal synthesis; structure characterization; photocatalytic activity; 2,4,6-tribromophenol

In the past two decades, mesoporous TiO_2 (M-TiO_2) with a large pore size and distinct mesostructure has attracted attention due to its outstanding photocatalytic activity for the decontamination of hydrophobic organic pollutants in water and air environment [1–6] and other fields [7]. However, the synthesis of M-TiO_2 is still a challenge due to difficulties in the rapid optimization of the synthesis conditions such as the method and parameters [8–13], e.g. the titanium source, acid catalyst, and ligand complexation reagents, etc. Among these methods, the sol-gel procedure is the simplest method to prepare M-TiO_2, which can be used with [10–14] or without [15,16] addition of structural directing reagents. In fact, the utilization of templates allows the forming of long-ranged 3D nanosize network materials with a well defined mesoporous structure [17,18]. Many different surfactant templates, such as neutral [19–21] and ionic surfactants [22,23] have been used to synthesize mesoporous materials based on different organic-inorganic interactions. Some well-defined M-TiO_2 have been successfully synthesized by using different structural directing reagents [17,24–26]. In our previous works, two non-ionic surfactants, amphiphilic triblock copolymers (Pluronic P123) [27] and polyethylene glycol (PEG) [10], were selected to synthesize a well-defined mesostructure and improve the photocatalytic activity, respectively. The mesostructure and the photocatalytic activity depended not only on the selected template structure but also its molecular weight. Thus, another surfactant template, polypropylene glycol (PPG), which has a very similar microstructure to both P123 and PEG, was also used to prepare M-TiO_2 photocatalysts because there are very few references on the synthesis of TiO_2 using PPG as the structural directing reagent [28].

In this study, M-TiO_2 samples with large pores and narrow

Received 31 March 2011. Accepted 16 May 2011.
*Corresponding author. Tel:+86-20-85291501; E-mail: antc99@gig.ac.cn
This work was supported by the National Natural Science Foundation of China (21077104), Knowledge Innovation Program of Guangzhou Institute of Geochemistry, CAS (GIGCX-10-01), and the Science and Technology Project of Guangdong Province, China (2009A030902003, 2009B030400001, and 2009B091300023).
This is contribution No. IS-1356 from GIGCAS.

DOI: 10.1016/S1872-2067(10)60241-0

pore size distributions were prepared using a hydrothermal sol-gel method, and used for the removal of hydrophobic organic pollutants from wastewater. The focus was on the tuning of the mesostructure of the M-TiO_2 and enhancing its photocatalytic activity by changing the synthesis conditions with the use of PPG as template. To obtain robust M-TiO_2 photocatalysts, the factors of whether a hydrothermal treatment was used, content of the template, and calcination temperature were optimized. The photocatalytic activities of the M-TiO_2 samples prepared were evaluated by using a typical brominated flame retardant, 2,4,6-tribromophenol (TBP), as a model organic pollutant in water.

1 Experimental

1.1 Preparation of M-TiO_2

Mesoporous TiO_2 was prepared via a hydrothermal sol-gel method reported in our previous papers [10,27]. In a typical synthesis, 5 g of titanium butoxide (chemical grade regent, Qiangsheng Chemical Ltd., China) was added dropwise to 20 ml of 20% HAc (analytical grade) aqueous solution (v/v) under vigorous stirring. The resulting mixture was sealed and stirred for 4 h to obtain solution A. A known content of liquid PPG (analytical grade) with the molecular weight of 1000 (designated as PPG 1000) was dissolved in 20 ml ethanol (analytical grade) under vigorous stirring to obtain solution B, where 0%, 5%, 10%, 20%, and 30% (v/v) PPG ethanol solution were used to evaluate the effect of the content of PPG. Solution B was added dropwise to solution A, and the final mixed solution was sealed, stirred for 24 h at room temperature, and hydrothermally treated in a Teflon sealed container at 120 °C for 48 h. Finally, the obtained mixture was filtered with a 0.22 μm filter and the filtrated colloid was air dried at 80 °C overnight, and then calcined at different temperatures for 2 h. To investigate the effect of calcination temperature, the samples prepared were calcined at 300, 350, 400, 450, and 500 °C for 2 h. All solutions were prepared using deionized and double distilled water.

1.2 Characterization of M-TiO_2

The X-ray diffractometer (XRD) was a Rigaku D/MAX-2200 VPC using Cu K_α radiation (λ = 0.15418 nm). It was used at a scanning speed of 5°/min to characterize the crystal composition of the M-TiO_2. Thermogravimetric-differential thermogravimetric (TG-DTG) analysis was carried out using a Netzsch STA 409 PC system. A scanning electron microscope (SEM, SU-1500) was used with an accelerating voltage of 200 kV to determine the morphology. A Micromeritics ASAP 2010 system was used to measure the adsorption and desorption isotherms.

1.3 Photocatalytic activity

Photocatalytic experiments were carried out in a 160 ml Pyrex glass chamber with a jacket. A 125 W high pressure Hg lamp that emits radiation with a maximum at 365 nm (GGZ125, Shanghai Yaming Lighting Co., Ltd., China) was used as the light source. The reaction temperature was kept at (27±2) °C by the continuous circulation of water in the jacket around the reactor. Reaction suspensions were prepared by adding 0.225 g of M-TiO_2 photocatalyst powder into 150 ml TBP (100 μmol/L) aqueous solution under vigorous stirring. Prior to irradiation, all reaction suspensions were stirred in the dark for 30 min to establish adsorption-desorption equilibrium. Once the concentration of TBP had stabilized, the sample was irradiated with UV light to start the photocatalysis. Subsequently, 2 ml reaction suspension was collected and filtered through 0.22 μm Millipore filter at fixed intervals. The concentrations of TBP in the solution were determined by high pressure liquid chromatography (HPLC) with a UV detector (λ = 286 nm) [10]. The mobile phase was optimized as 55 vol% acetonitrile and 45 vol% water pumped at 1 ml/min. An Agilent 1200 HPLC was used to measure the TBP concentration using an Agilent C18 reverse-phase column (150 mm × 4.6 mm, 5 μm) at 35 °C.

2 Results and discussion

2.1 XRD analysis

The wide angle XRD patterns of M-TiO_2 photocatalysts prepared under different conditions are shown in Fig. 1. The XRD patterns exhibited similar main diffraction peaks for all the photocatalysts at 2θ = 25.3°, 37.2°, 48.9°, 54.0°, 55.3°, 62.4°, and 68.7°. These peaks were indexed to (101), (004), (200), (105), (211), (204), and (112) indicating that anatase was the only crystalline phase in the samples. Hydrothermal treatment is widely employed as an efficient method to control the phase composition and morphology of M-TiO_2 [10]. The XRD data of M-TiO_2 synthesized with and without a hydrothermal treatment are compared in Fig. 1(a). There was not much difference between the samples except that the mean crystallite sizes of the M-TiO_2 prepared without the hydrothermal treatment was 20.1 nm, which decreased to 15.3 nm with the hydrothermal treatment (Table 1, entries 3 and 6). The sizes were calculated from the broadening of the (101) XRD peaks of the anatase phase using the Scherrer formula [29,30].

The effect of the calcination temperatures on the composition of M-TiO_2 has been extensively studied because of its prominent effect on both the crystalline phase and the pore structure of the resulting photocatalysts [8,31]. To optimize the calcination temperatures, the simultaneous TG and DTG profiles illustrated in Fig. 2 were used. With the increase of cal-

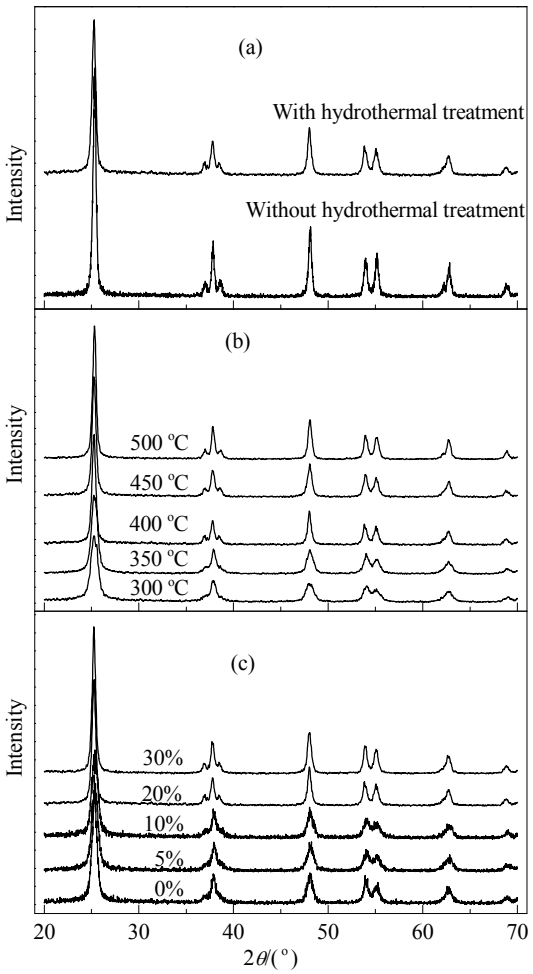

Fig. 1. XRD patterns of the M-TiO_2 samples. (a) Prepared with different treatment methods (PPG content, 20%; calcination at 400 °C for 2 h; hydrothermal treatment time, 48 h); (b) Prepared at different calcination temperatures (PPG content, 20%; hydrothermal treatment time, 48 h); (c) Prepared with different PPG contents (hydrothermal treatment time, 48 h; calcination at 400 °C for 2 h).

cination temperature, the mass loss curve (TG) decreased slowly before 260 °C, suggesting the evaporation of acetic acid and the dehydration of adsorbed water from the sample.

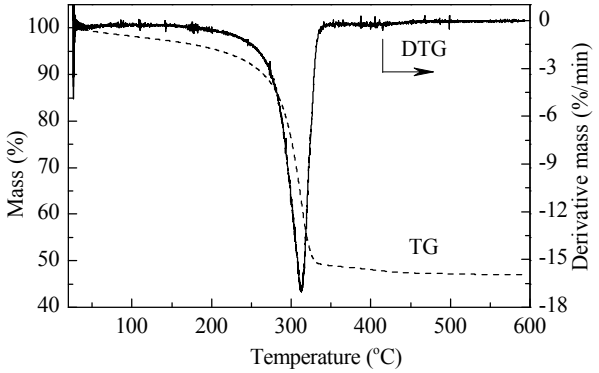

Fig. 2. Simultaneous TG and DTG curves for the TiO_2 sample prepared with 20% PPG content and a hydrothermal treatment for 48 h.

In this temperature range, a total of 10.0% mass loss was observed. With the further increase of the temperature to 330 °C, a significant mass loss of 50.5% occurred, and the highest rate of mass loss (DTG) was reached around 315 °C. This larger mass loss was mainly due to the partial combustion of the added PPG template. Thus it may be concluded that most of the PPG template decomposed after 330 °C. Another small mass loss of 2.5% was seen in the subsequent 125 °C interval, indicating a slight change of the microstructure of the prepared M-TiO_2. As a check on the change of the microstructure, the wide angle XRD patterns of the M-TiO_2 photocatalysts prepared at different calcination temperatures were also obtained. These are illustrated in Fig.1(b). With increasing calcination temperature, the diffraction peak intensity became stronger and the peak width became much narrower. It was deduced from the XRD patterns (Fig.1(b)) that there was a remarkable increase of M-TiO_2 crystallite sizes from 8.1 to 17.8 nm when the calcination temperature was increased from 300 to 500 °C (Table 1, entries 1–5). The pure anatase phase of M-TiO_2 was still maintained even at 500 °C.

The wide angle XRD patterns of M-TiO_2 prepared with different contents of PPG template are shown in Fig. 1(c). With increasing content of PPG, the diffraction peak intensity became weaker first and then stronger, while the peak width

Table 1 Structural parameters of M-TiO_2 prepared under different conditions

Entry	Calcination temperature (°C)	Concentration of PPG (%)	Crystalline size[a] (nm)	A_{BET}[b] (m^2/g)	Mean pore size[c] (nm)	Total volume[d] (cm^3/g)
1	300	20	8.1	136	13.0	0.37
2	350	20	9.1	103	13.1	0.35
3	400	20	15.3	116	15.3	0.30
4	450	20	15.9	66	15.5	0.23
5	500	20	17.8	53	14.9	0.20
6[e]	400	20	20.1	39	16.7	0.14
7	400	0	13.0	91	9.2	0.22
8	400	5	10.0	123	15.3	0.41
9	400	10	9.8	126	19.0	0.43
10	400	30	17.8	45	15.3	0.15

[a]Calculated by the Scherrer formula. [b]BET surface area calculated from the linear part of the BET plot. [c]Estimated using the desorption branch of the isotherm. [d]Single-point total pore volume of pores at $p/p_0 = 0.99$. [e]Without hydrothermal treatment.

became wider first and then got narrower. The weakest diffraction peak intensity and the widest peak width were obtained with 10% PPG, which gave the smallest grain size. It was further confirmed from the data in Table 1 that the crystallite size of M-TiO_2 was 13.0 nm without PPG added as template, while with the increase of PPG content, the crystallite sizes first slightly decreased to 9.8 nm at 10% PPG content, and then further increased to 15.3 and 17.8 nm at 20% and 30% PPG content, respectively. This indicated that the added content of template reagent was very important in M-TiO_2 preparation. This was because the PPG surfactant has different complexion structures with water molecules and resulted in different template structures in aqueous solutions with their different contents, leading to different pore structures and crystalline sizes of the TiO_2. In this system, the optimal added content of the PPG template was 10%.

2.2 N_2 adsorption-desorption measurement

The N_2 adsorption-desorption isotherms and Barrett-Joyner-Halenda (BJH) pore size distributions of representative samples are displayed in Fig. 3. Figure 3(a) shows the N_2 adsorption-desorption isotherms and BJH pore size distribution profiles of the samples prepared with and without hydrothermal treatment. Both isotherm curves had Type IV shape with a small H1 hysteresis loop, implying the existence of mesopores seen at the high relative pressure range between 0.80 and 0.99 (Type IV) [32,33]. Although both samples were mesoporous materials, the N_2 adsorbed quantity of M-TiO_2 prepared with a hydrothermal treatment was much higher, indicating more abundant mesopores in the hydrothermally treated M-TiO_2. The maximum adsorption peak at 15.3 nm for the hydrothermal prepared M-TiO_2 was much higher and narrower than that without a hydrothermal treatment which peaked at 16.7 nm. This indicated that the hydrothermal treatment suppressed the aggregation of the crystallite particles and increased the uniformity of the mesopores, but did not enlarge the pore size [10]. The BET surface areas and other structure parameters of M-TiO_2 prepared with or without hydrothermal treatment are also summarized in Table 1. For the sample without hydrothermal treatment, the BET surface area was 39 m^2/g and the mean pore size was 16.7 nm, while

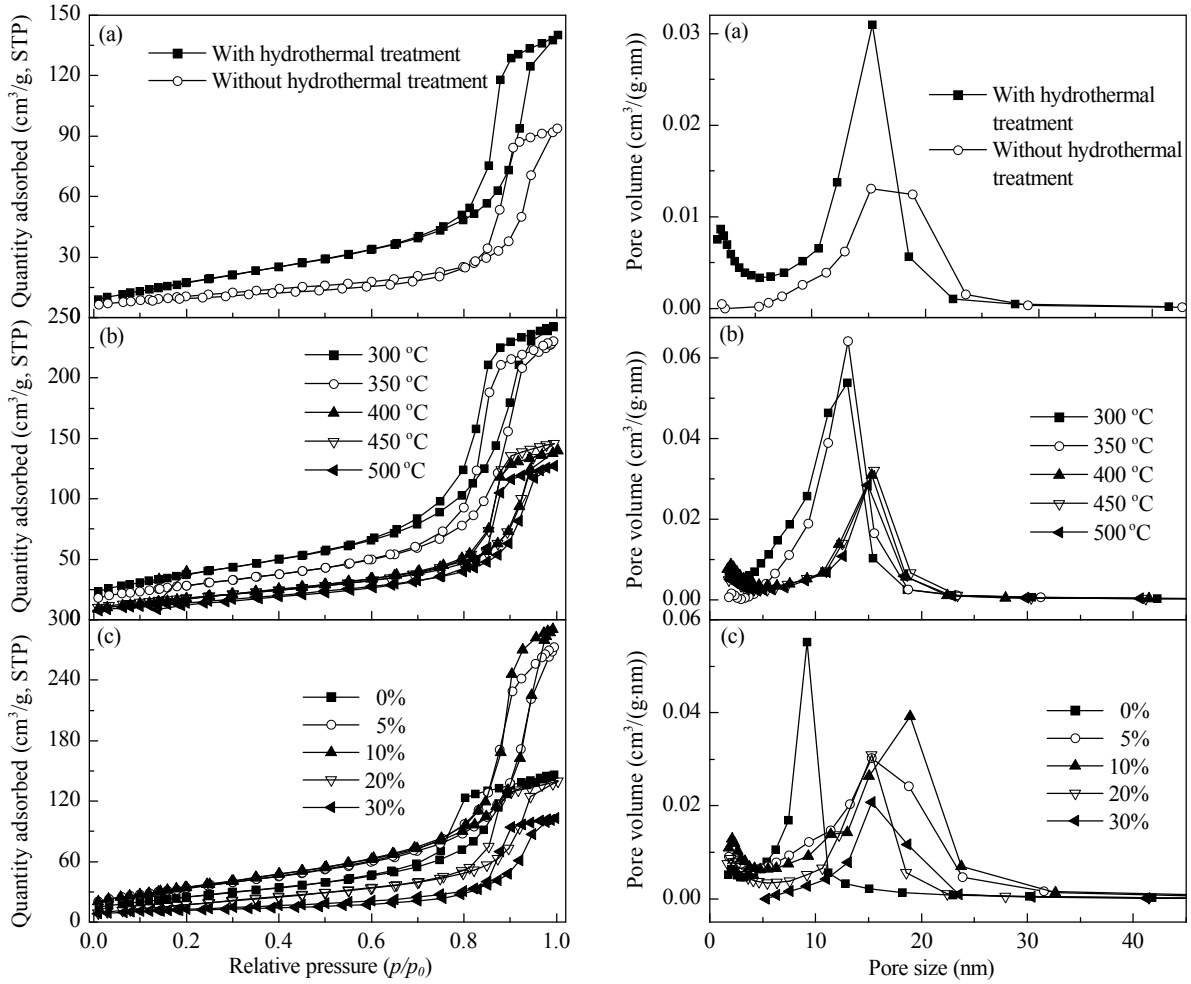

Fig. 3. N_2 adsorption-desorption isotherms and BJH pore size distribution of M-TiO_2. (a) Prepared by different treatment methods (PPG content, 20%; calcination at 400°C for 2 h; treatment time, 48 h); (b) Prepared at different calcination temperatures (PPG content, 20%; hydrothermal treatment time, 48 h); (c) Prepared with different PPG contents (hydrothermal treatment time, 48 h; calcination at 400 °C for 2 h).

with hydrothermal treatment, the BET surface areas and mean pore size were 116 m^2/g and 15.3 nm, respectively (Table 1, entries 3 and 6). The total pore volume of 0.30 cm^3/g for the sample with hydrothermal treatment was larger than that of 0.14 cm^3/g without hydrothermal treatment. This implied that the hydrothermally treated M-TiO_2 sample contained more and smaller uniform mesopores. This may be due to that the hydrothermal treatment can speed up the reaction equilibrium and decrease the pore size with the addition of PPG template.

Figure 3(b) shows the N_2 adsorption-desorption isotherms and pore size distribution of hydrothermally prepared M-TiO_2 with different calcination temperatures. All isotherms had Type IV curve characteristics with a small H1 hysteresis loop, indicating ordered cylindrical pores [33]. The N_2 adsorbed amounts of M-TiO_2 with different calcination temperatures can be divided into two different groups. The N_2 adsorbed amounts of M-TiO_2 calcined at 300 or 350 °C were almost twice as large as those of the samples calcined at 400, 450, and 500 °C. This indicated that the mesoporous structure of the prepared M-TiO_2 was preserved very well before 350 °C, and collapsed with the burning of the template when the calcination temperature was further increased. This was confirmed by the TG and DTG experiments described earlier that most of the template in the M-TiO_2 samples was combusted around 315 °C and before 330 °C. Similarly, the pore size distributions of M-TiO_2 samples with different calcination temperatures were also grouped into two types. For the samples calcined at 300 or 350 °C, the pore size distribution peaked at 13.0 and 13.1 nm, respectively. This was due to the mesoporous structure consolidation as a result of the improved PPG template to form uniformed mesopores. However, with further increase of the calcination temperatures to 400 and 500 °C, the mesoporous structure was partially destroyed because of the combustion of the PPG template, and thus the pore size distribution became less uniform and the peak was much larger at 15.3 and 14.9 nm due to the collapse of the mesoporous structure and the aggregation of the nano-scale TiO_2 particles. Furthermore, Table 1 with the data of the specific surface areas and total volumes also confirmed this trend. With increased calcination temperature, the specific surface area and the total volume decreased slightly from 136 m^2/g and 0.37 cm^3/g to 103 m^2/g and 0.35 cm^3/g at 350 °C, then rapidly to 53 m^2/g and 0.20 cm^3/g at 500 °C. These data can be explained by that with the increase of calcination temperature, the particle size grew much larger due to the physical aggregation of TiO_2 particles, leading to the decrease of the surface area and pore volume, even when the mean pore size of particles increased slowly (Table 1).

Figure 3(c) also shows the N_2 adsorption-desorption isotherms and pore size distribution curves of M-TiO_2 samples prepared with different PPG contents. All isotherms had Type IV profiles with a H1 hysteresis loop except for the sample prepared without PPG, which exhibited a H2 hysteresis loop. These indicated that all the samples were mesoporous TiO_2 although they had different hysteresis loops. Without the use of the PPG template, the N_2 adsorbed amount was much lower at 146.4 cm^3/g, and the M-TiO_2 sample consisted of many small ink bottle pores with narrow necks and wide bodies [32,33]. However, the M-TiO_2 sample was composed of agglomerates of approximately uniform spheres with a narrow range for the pore size distribution [10]. With the addition of the PPG template, the N_2 adsorbed amount increased first to 272.7 and 290.4 cm^3/g at 5% and 10% PPG contents, and then decreased to 140.0 and 102.7 cm^3/g at 20% and 30% PPG contents. The textural and structural parameters of the samples are summarized in Table 1. With increasing PPG content, the BET surface area and mean pore size increased first from 91 m^2/g and 9.2 nm at 0% PPG content to 126 m^2/g and 19.0 nm at 10% PPG content, and then slowly decreased to 45 m^2/g and 15.3 nm at 30% PPG content. On the other hand, the total volume also increased first from 0.22 cm^3/g at 0% PPG content to 0.43 cm^3/g at 10% PPG content, and then decreased to 0.15 cm^3/g at 30% PPG content. All these experimental results indicated that the content of PPG template has an optimal range to prepare large area and active M-TiO_2, and 10% was the best content of the PPG template in this system. This may be due to the linear chain structure of the PPG with a block construction of -C-C-O- in which the oxygen has strong nucleophilicity. Thus, a series of PPG molecules will connect with each other end to end when the PPG content is high, and some TiO_2 gets wrapped in it. The oxygen and the Ti form a crown ether type complex through the coordination bond and are dispersed in the system.

2.3 Morphology observation

SEM images of the M-TiO_2 prepared with and without hydrothermal treatment are shown in Fig. 4. Each sample consists of the aggregation of nanoparticles with particle sizes of 10 to 20 nm. The particle size increased with increasing calcination temperature for the catalysts with hydrothermal treatment for 48 h, which is in good agreement with the results calculated from the XRD patterns. Comparing the SEM images of the M-TiO_2 prepared with (Fig. 4(b)) and without (Fig. 4(d)) hydrothermal treatment and calcined at the same 400 °C for 2 h, it can be seen that the SEM image of those with the hydrothermal treatment exhibited a much clearer pore structure and smaller particle sizes than those without the hydrothermal treatment.

It can also be easily seen from Fig. 4(a) that the M-TiO_2 prepared at 300 °C comprised very indistinct particles without any apparent mesoporous structure. This was due to the partial combustion of the PPG template. On increasing the temperature to 400 °C, the M-TiO_2 prepared (Fig. 4(b)) had a much clearer porous appearance with a very uniform array of nanoparticles because of the complete combustion of the PPG

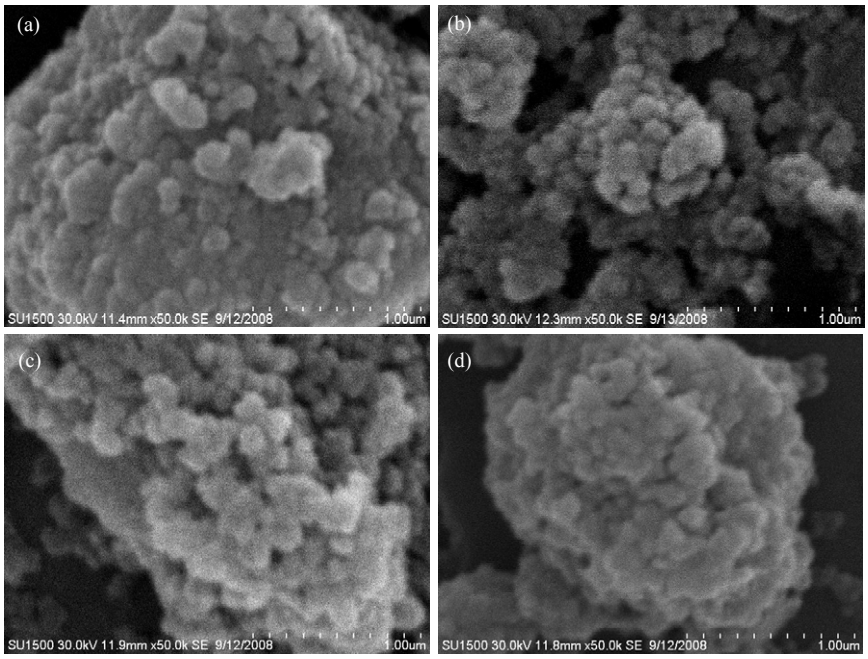

Fig. 4. SEM images of M-TiO_2 prepared at different calcination temperatures. (a) 300 °C; (b) 400 °C; (c) 500 °C with a hydrothermal treatment for 48 h; (d) 400 °C without a hydrothermal treatment.

template. On further increasing of the temperature to 500 °C, the porous appearance become blurred again, and the particle sizes were much larger (Fig. 4(c)) due to the partial collapse of porous structure, aggregation, and rebuilding of the nanoparticles resulting from the burning of the PPG template.

2.4 Photocatalytic activity of M-TiO_2

The photocatalytic activities of the M-TiO_2 photocatalysts prepared with different calcination temperatures and with different PPG contents were assessed using TBP as a model organic compound. There was not much difference in the photocatalytic degradation kinetics of TBP with M-TiO_2 prepared with or without a hydrothermal treatment although the structure characteristics were quite different for these two catalysts. In contrast to the influence of the treatment method, the calcination temperature and PPG content influenced the photocatalytic degradation activities of the M-TiO_2 photocatalysts were also investigated (Fig. 5).

Figure 5(a) shows the degradation profiles of TBP with M-TiO_2 prepared with different calcination temperatures. For a reaction time of 60 min, the TBP degradation efficiency first increased from 91.0% at 300 °C to 100% as the calcination temperature increased to 350 and 400 °C, and then decreased to 95.0% and 96.0% when the calcination temperature was further increased to 450 and 500 °C. As previously discussed, this can be explained by that with the increase of the calcination temperature, the PPG surfactants used as the template in M-TiO_2 was partially burned out before 300 °C, and the burning was complete after 350 °C. The mesoporous structure of the prepared M-TiO_2 was well preserved when the calcination temperatures were less than 400 °C. The improved anatase phase structure and well maintained mesopores contributed to the enhancement of photocatalytic activity of the M-TiO_2 obtained by calcination at 400 °C. The low activity of the photocatalyst calcined at 300 °C could be due to the inhibiting

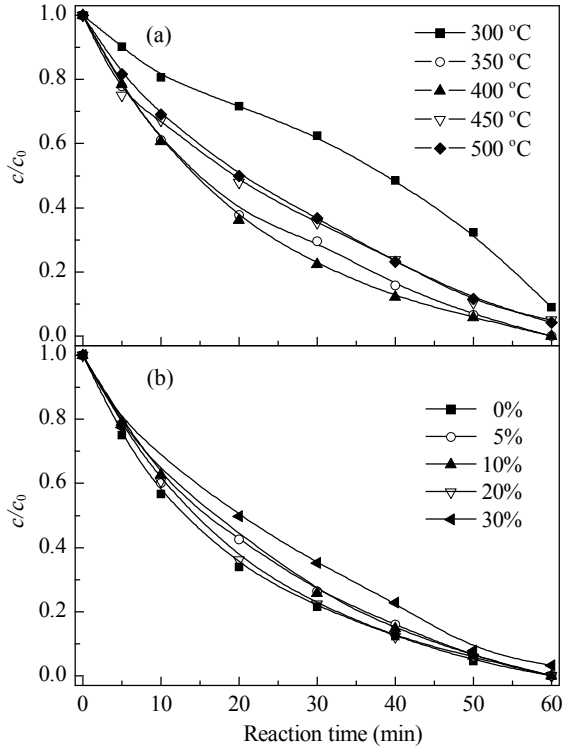

Fig. 5. Degradation of TBP using M-TiO_2 photocatalysts prepared at different calcination temperatures (a) and with different PPG contents (b).

effect of the partly-burnt carbonaceous residues. The decrease of the photocatalytic degradation efficiency for the catalyst calcined at 500 °C was due to the collapse of the mesoporous structure and the decrease in the BET surface area and total volume of the M-TiO_2. This trend was confirmed very well by the structure data shown in Table 1. When the thermal treatment temperature increased from 300 to 500 °C, the crystallite size increased from 8.1 to 17.8 nm, while the BET areas decreased from 136 to 53 m^2/g.

Figure 5(b) presents the degradation curves of TBP using the M-TiO_2 samples prepared with different concentrations of PPG. All the degradation efficiencies were almost 100% except for the M-TiO_2 prepared at 30% PPG contents. This indicated that the addition of PPG template facilitated the growth of the mesoporous structure and limited the aggregation of the nanoparticles, which improved the activity of the M-TiO_2 photocatalyst. This is in good agreement with the structure data discussed earlier. The lower photocatalytic efficiency may be partially attributed to the increase of crystallite size and the decrease of the mean pore size as well as the BET surface area and total volume. From Table 1, it can be concluded that with increasing PPG content, the BET surface area and mean pore size of M-TiO_2 first increased and then decreased. These variations may reflect some change in the configuration of the ethylene chain in the PPG solution with PPG content. Thus, we can conclude that the photocatalytic activities of the photocatalysts were not only affected by the structure parameters, such as the surface area, pore volume, and pore size, but also depended on the crystalline phase of the M-TiO_2 photocatalyst and its particle size [7].

3 Conclusions

Mesoporous TiO_2 photocatalysts with a regular channel structure, large mean pore sizes, and high specific surface areas were synthesized by using PPG as template. The effects of preparation method, content of templating reagent, and calcination temperature on the microstructure and photocatalytic activity were investigated. The relationship between the microstructure of the mesoporous TiO_2 samples and photocatalytic activity was studied with the photocatalytic degradation of TBP in water. The best catalyst was the sample calcined at 400 °C, with the PPG content of 20%, and with a hydrothermal treatment, which gave the complete degradation of 100 μmol/L TBP with 1 h irradiation.

References

1 Pan J H, Dou H Q, Xiong Z G, Xu C, Ma J Z, Zhao X S. *J Mater Chem*, 2010, **20**: 4512
2 An T C, Sun L, Li G Y, Gao Y P, Ying G G. *Appl Catal B*, 2011, **102**: 140
3 Sheng Q R, Yuan S, Zhang J L, Chen F. *Microporous Mesoporous Mater*, 2006, **87**:177
4 Wang X C, Yu J C, Ho C M, Hou Y D, Fu X Z. *Langmuir*, 2005, **21**: 2552
5 Yu J G, Su Y R, Cheng B. *Adv Funct Mater*, 2007, **17**: 1984
6 Peng T Y, Zhao D, Dai K, Shi W, Hirao K. *J Phys Chem B*, 2005, **109**: 4947
7 Taguchi A, Schuth F. *Microporous Mesoporous Mater*, 2005, **77**: 1
8 Sun L, An T C, Wan S G, Li G Y, Bao N Z, Hu X H, Fu J M, Sheng G Y. *Sep Purif Technol*, 2009, **68**: 83
9 Yu J G, Yu J C, Leung M K P, Ho W K, Cheng B, Zhao X J, Zhao J C. *J Catal*, 2003, **217**: 69
10 An T C, Liu J K, Li G Y, Zhang S Q, Zhao H J, Zeng X Y, Sheng G Y, Fu J M. *Appl Catal A*, 2008, **350**: 237
11 Yuan S, Sheng Q R, Zhang J L, Yamashita H, He D N. *Microporous Mesoporous Mater*, 2008, **110**: 501
12 Choi H, Sofranko A C, Dionysiou D D. *Adv Funct Mater*, 2006, **16**: 1067
13 Yu J G, Zhang L J, Cheng B, Su Y R. *J Phys Chem C*, 2007, **111**: 10582
14 Fei H L, Liu Y P, Li Y P, Sun P C, Yuan Z Y, Li B H, Ding D T, Chen T H. *Microporous Mesoporous Mater*, 2007, **102**: 318
15 Drisko G L, Luca V, Sizgek E, Scales N, Caruso R A. *Langmuir*, 2009, **25**: 5286
16 Kulkarni D G., Murugan A V, Viswanath A K, Gopinath C S. *J Nanosci Nanotechnol*, 2009, **9**: 371
17 Mohammadi M R, Fray D J, Cordero-Cabrera M C. *Sensor Actuat B*, 2007, **124**: 74
18 Zhou J F, Zhou M F, Caruso R A. *Langmuir*, 2006, **22**: 3332
19 Mokaya R, Zhou W Z, Jones W. *Chem Commun*, 1999: 51
20 Zhao D, Huo Q, Feng J, Chmelka B F, Stucky G D. *J Am Chem Soc*, 1998, **120**: 6024
21 Luan Z, Cheng C, Zhou W, Klinowski J. *J Phys Chem*, 1995, **99**: 1018
22 Lim M H, Blanford C F, Stein A. *J Am Chem Soc*, 1997, **119**: 4090
23 Yang H, Coombs N, Ozin G A. *Nature*, 1997, **386**: 692
24 Antonelli D, M Y J Y. *Angew Chem*, *Int Ed*, 1995, **34**: 2014
25 Sertchook H, Elimelech H, Makarov C, Khalfin R, Cohen Y, Shuster M, Babonneau F, Avnir D. *J Am Chem Soc*, 2007, **129**: 98
26 Hirashima H, Imai H, Balek V. *J Non-Cryst Solids*, 2001, **285**: 96
27 Liu J K, An T C, Li G Y, Bao N Z, Sheng G Y, Fu J M. *Microporous Mesoporous Mater*, 2009, **124**: 197
28 Li Y J, Ma M Y, Wang X H, Li Z P. *Surf Coat Technol*, 2010, **204**: 1353
29 Zhang M L, An T C, Hu X H, Wang C, Sheng G Y, Fu J M. *Appl Catal A*, 2004, **260**: 215
30 Klug H P, Alexander L E. New York: Wiley, 1974. 618
31 Ding X J, An T C, Li G Y, Zhang S Q, Chen J X, Yuan J M, Zhao H J, Chen H, Sheng G Y, Fu J M. *J Colloid Interf Sci*, 2008, **320**: 501
32 Sing K S W, Everett D H, Haul R A W, Moscou L, Pierotti R A, Rouquerol J, Siemieniewska T. *Pure Appl Chem*, 1985, **57**: 603
33 Kruk M, Jaroniec M. *Chem Mater*, 2001, **13**: 3169